

In order to reduce the ripple due to the active filter's switching operation, it is essential to connect the active filter to the network through a passive filter usually of the first order (L_f, R_f). On the DC side, a capacity C is connected in parallel to store energy. The capacity serves as a voltage source and allows the operation of the static converter as a rectifier or inverter.

The generation of reference signals is ensured by the p-q method. The switching times of the inverter are generated by the hysteresis control method where two techniques will be considered: a hysteresis current control with fixed band and another with fuzzy band. In order to ensure effective DC voltage control, a fuzzy logic controller is used in place of a PI regulator

PQ theory based on ADALINE algorithm extraction

Generally, the extraction of harmonic powers is carried out in this technique by two low-pass filters. In order to be able to achieve good power separation and thus provide an exact set point for the SAPF modulation technique, the two low-pass filters will be replaced by two ADALINE-type neural networks (Fig.2.).

The first step of the harmonic extraction process using ADALINE is to generate the input vector x_i of the ADALINE; this vector is constituted of a combination of Sine and Cosine waves at the frequency of the fundamental and the most dominant harmonics. Then, sensing the waveform of the signal to process and feeding it as a target result. Later, random widths vector w_i is initiated, and the ADALINE is lunched. During every iteration the ADALINE force its output to converge toward the target signal by constantly updating the widths vector using the LMS algorithm (Fig.3.).[10].

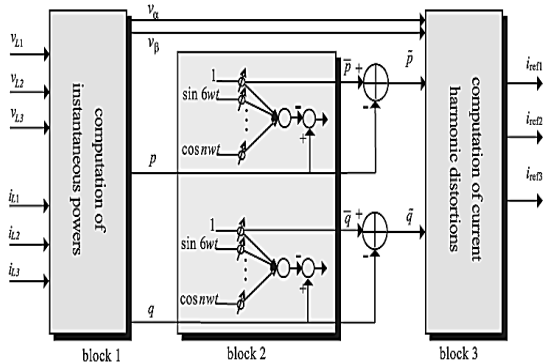


Fig.2. PQ theory based on two ADALINEs algorithm extraction

In order to estimate the real and imaginary instantaneous powers, it is possible to decompose the currents I_{sabc} and voltages V_{sabc} of an electric network into a Fourier series as follows[11]:

$$(1) \quad I_{sabc}(t) = \sum_{n=1 \dots N} \begin{bmatrix} I_{n1} \cos n(\omega t - \alpha) - \\ I_{n2} \sin n(\omega t - \alpha) \end{bmatrix}$$

$$(2) \quad V_{sabc}(t) = \sum_{n=1 \dots N} [V_{n1} \cos n\omega t - V_{n2} \sin n\omega t]$$

Where: ω – fundamental frequency of the electrical network, I_{n1} and I_{n2} – amplitudes of the sinus and cosine components of the network current, α – phase angle between current and voltage, V_{n1} and V_{n2} – amplitudes of the sine and cosine components of the main voltages. Using a frequency analysis, the expressions (3) of the instantaneous powers is developed as follows:

$$(3) \quad \begin{cases} p = \bar{p} + \tilde{p} \\ q = \bar{q} + \tilde{q} \end{cases}$$

$$(4) \quad \begin{cases} p(t) = p_1 \cos \alpha + p_5 \cos(6\omega t - 5\alpha) \\ - p_7 \cos(6\omega t - 7\alpha) - \dots \\ q(t) = -q_1 \sin \alpha - p_5 \sin(6\omega t - 5\alpha) \\ - p_7 \sin(6\omega t - 7\alpha) + \dots \end{cases}$$

$p_1 \cos \alpha$ and $-q_1 \sin \alpha$ represent the continuous parts of p and q respectively. The rest of terms is the alternative parts. To extract estimate active and reactive powers, two ADALINE are developed, where the inputs are sinusoidal functions that correspond to each harmonic order in the mathematical developments shown in equations (4). The Fourier analysis can express the instantaneous real and imaginary powers in the general case as follows:

$$(5) \quad f(t) = A_0 + \sum_{n=1 \dots N} \begin{bmatrix} A_{n1} \cos(n\omega t - (n-1)\alpha) + \\ A_{n2} \cos(n\omega t - (n+1)\alpha) + \\ B_{n1} \sin(n\omega t - (n-1)\alpha) + \\ B_{n2} \sin(n\omega t - (n+1)\alpha) \end{bmatrix}$$

Where: A_0 – continuous part, A_{n1} , A_{n2} and B_{n1} , B_{n2} – amplitudes of the sinus and cosines terms respectively. The vector representation of equation (5) is given by:

$$(6) \quad f(t) = W^T \cdot X(t)$$

where: W^T – weight vector of the network, $X(t)$ – input vector of the network.

$$(7) \quad W^T = [A_0 A_{11} A_{12} B_{11} B_{12} \dots A_{N1} A_{N2} B_{N1}]$$

$$(8) \quad X^T = \begin{bmatrix} 1 \\ \cos(6\omega t - 5\alpha) \\ \sin(6\omega t - 5\alpha) \\ \cos(6\omega t - 7\alpha) \\ \sin(6\omega t - 7\alpha) \\ \dots \\ \dots \\ \dots \\ \cos(n\omega t - (n-1)\alpha) \\ \sin(n\omega t - (n-1)\alpha) \\ \cos(n\omega t - (n+1)\alpha) \\ \sin(n\omega t - (n+1)\alpha) \end{bmatrix}$$

The equation (6) can then be implemented by the ADALINE configuration illustrated by Fig.3. where W^T is the weight vector of the network and $X(t)$ its input. Figure 4, shows this instantaneous power topology for p reel power (which is the same topology for q imaginary power) to be compensated by two ADALINE as illustrated in the figure below.

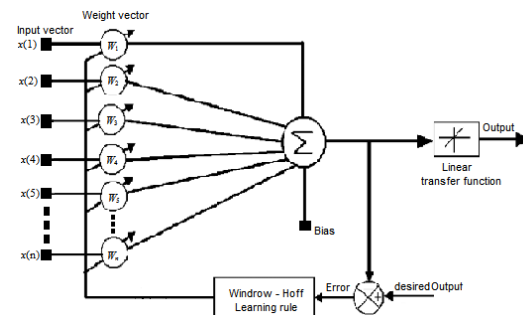


Fig.3. The general network topology of an ADALINE

Hysteresis current control with fixed and fuzzy band

Switching times of the SAPF are generated using two modulation techniques: the hysteresis current control with fixed band (Fig.4) and fuzzy band (Fig.5).

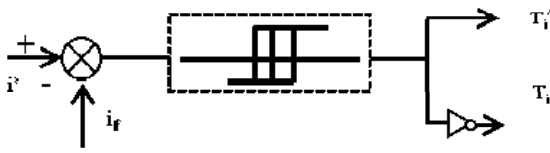


Fig.4. Principle diagram of the hysteresis current control with fixed band

The hysteresis fixed band constitutes a major disadvantage for this control structure. The switching frequency depends essentially on the derivative of the set point current. The amplitude of the derivative is not mastered and the switching frequency is not fixed[8], [12].

This point can be particularly penalizing in the case of high power systems where the switching frequency is limited to values of the order of KHz because of the characteristics of the electronic power components. New techniques based on the same concept have been developed to improve performance of the hysteresis current control strategy: The most popular are the auto-adaptive band hysteresis, and the fuzzy auto-adaptive band hysteresis (figure 5)[12].

The current control with adaptive band hysteresis overcomes the problem of switching frequency variation, but this technique is sensitive to parametric variations in the SAPF. This is because this strategy control is based on the calculation of the hysteresis band so that the switching frequency remains constant[8]. Taking into account the parameters of the active filter (L_f , V_{dc}) as well as the reference current, the width of the band is regularly updated by the calculation algorithm making it possible to adapt it to the desired frequency.

$$(9) \quad HB = \frac{\alpha V_{dc}}{4f_c L_f} \left[1 - \frac{L_f^2}{\alpha^2 V_{dc}^2} \left(\frac{V_{s1}}{L_f} + \frac{di^*}{dt} \right) \right]$$

Fuzzy logic has been introduced to solve problems of conventional techniques of hysteresis current control. Current control with fuzzy hysteresis band is based on a dynamic tuning of the hysteresis band. This setting allows a constant switching frequency. The main advantage is the insensitivity of this control structure of the parametric variations of the SAPF.

The fuzzy hysteresis technique improves the performance

of the network compared to the fixed hysteresis strategy and has a good filtering quality with more sinusoidal network currents[13].

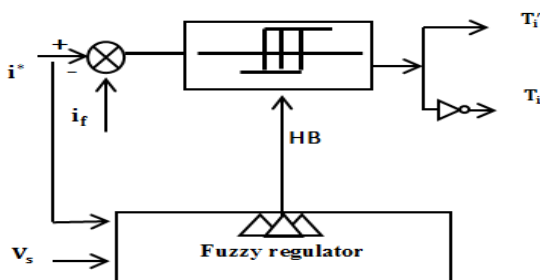


Fig.5. Hysteresis control with fuzzy auto adaptive band

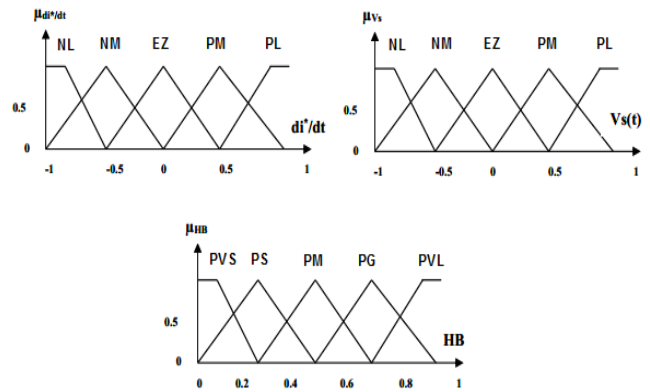


Fig.6. Membership functions of the input and output variables of the fuzzy inference system

As input to the fuzzy controller, the main voltage and the current reference slop can be selected. The hysteresis band magnitude is used as output. To determine the set of the linguistic values associated with each variable the following step is used. Each input variable is transformed into a linguistic size with five fuzzy subsets: PL is positive large, PM is positive medium, PS is positive small, EZ is zero, NL is negative large, NM is negative medium, and NS is negative small; for the output variable, HB, PVS is positive very small, PS is positive small, PM is medium positive, PL is positive large, and PVL is positive very large. The membership functions of the input and output variables are shown in Fig. 8 and the resulting inference rules are listed in Table1[8].

Table 1. Matrix of inferences

$\frac{di^*/dt}$ $V_s(t)$	NL	NM	EZ	PM	PL
NL	PS	PS	PM	PS	PS
NM	PS	PM	PG	PM	PS
EZ	PVS	PM	PVL	PM	PVS
PM	PS	PM	PG	PM	PS
PL	PS	PS	PM	PS	PS

Fuzzy DC voltage control

A fuzzy controller has been developed for controlling DC-link voltage and improves filtering performance of the SAPF. To do this, we have introduced the concept of fuzzy logic as shown in Figure 9[14]. A fuzzy logic controller is based on a collection of control rules governed by the compositional rule of inference applied to maintain the constant voltage across the capacitor by minimizing the error between the capacitor voltage and its reference voltage[15].

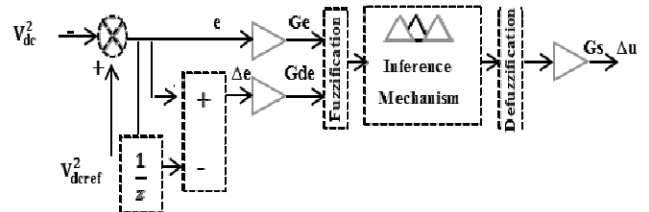


Fig.7. Structure of the DC voltage fuzzy control

The control law of the system is a function of the error and its variation:

$$(10) \quad \Delta u = f(e, \Delta e)$$

The most general form of this control law is defined as follows:

$$(11) \quad \Delta u(k+1) = \Delta u(k) + G_s \Delta u$$

The error and its variation are defined as follows:

$$(12) \quad \begin{cases} e(k) = G_e (V_{dref}^2(k) - V_{dc}^2(k)) \\ \Delta e(k) = G_{\Delta e} (e(k) - e(k-1)) \end{cases}$$

Where: $X(t)$ – input, k – Iteration number, Δu – command signal.

Table 2. Inference table of the fuzzy DC voltage controller

$e \backslash \Delta e$	NB	NM	NS	ZE	PS	PM	PB
NB	NB	NB	NM	NB	NM	NS	ZE
NM	NB	NM	NM	NM	NS	ZE	PS
NS	NM	NM	NS	NS	ZE	PS	PM
ZE	NB	NM	NS	ZE	PS	PM	PM
PS	NM	NS	ZE	PS	PS	PM	PM
PM	NS	ZE	PS	PM	PM	PM	PB
PB	ZE	PS	PM	PB	PM	PB	PB

Results and discussion

Simulation results were obtained under the Matlab \ Simulink environment and also using the Fuzzy toolbox. In order to show the advantages of Adaline Neural Network and fuzzy set theory to the SAPF control system, three comparative studies were carried out in this section: On the one hand, between the PI regulator of the SAPF DC voltage and a fuzzy logic controller, and on the other hand between the fixed band hysteresis and the fuzzy band modulation technique. The third study is the replacing of the two low-pass filters of RIIP method by two ADALINE networks for generation of reference currents of the SAPF, This is the Neural-RIIP (Real and Imaginary Instantaneous Powers) method. In order to further verify the effectiveness of the proposed control techniques, a load variation occurs from $t=0.1$ second (Fig.8). Figs.9, 10 shows the frequency spectrum of the load current before and after the load variation respectively. The THD of the line current is equal to 12.64%. We can see that the load variation has a negative effect on the value of the THD, since it goes from 9.02% to 12.64%. These spectral representations allow us to consider the 5th and the 7th harmonics as being the most dominant.

Table 3. Parameters of the studied system

Power grid				
Parameter	Source voltage	Frequency	source resistor	source inductance
Values	380 v	50 Hz	0.1 Ω	0.005mH
Non-linear load				
Parameter	Rectifier resistor	Rectifier inductance	Load inductance	Load resistor
Values	0.66 Ω	3mH	0.25mH	1 Ω
Shunt active power filter				
Parameter	filter inductance	Filter resistor	DC reference voltage	capacitor
Values	3mH	0.1 Ω	700v	2200uf

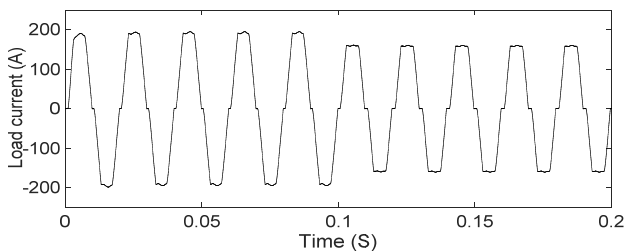


Fig.8. Waveform of the load current

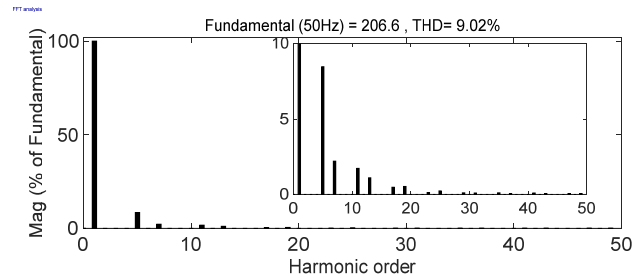


Fig.9. Frequency spectrum of load current before the load variation

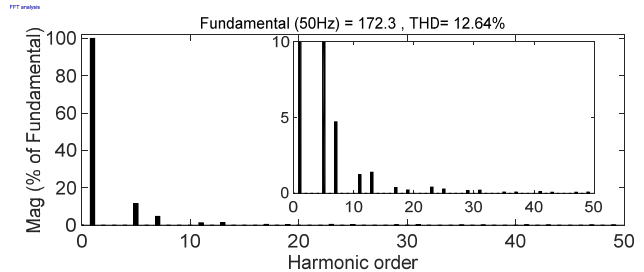


Fig.10. Frequency spectrum of load current after the load variation

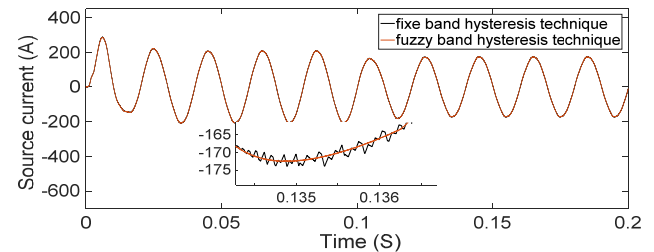


Fig.11. Waveform of the source current after filtering used low-pass filters

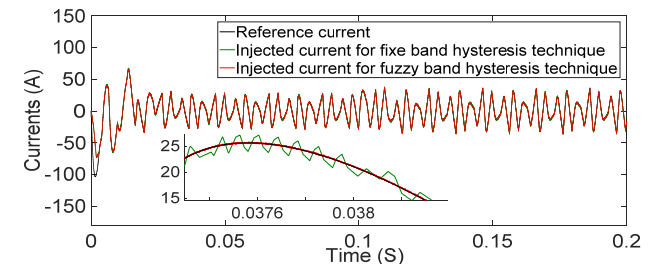


Fig.12. Injected current by the fixed band and fuzzy band hysteresis technique used low-pass. Filters

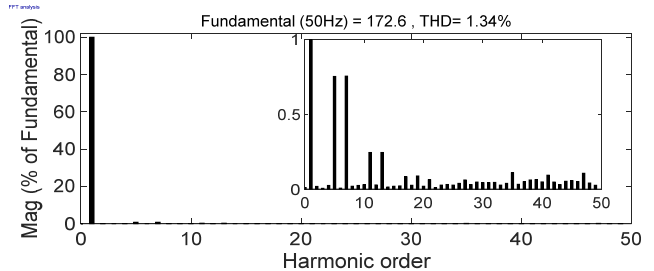


Fig.13. Frequency spectrum of source current for fixed band hysteresis and PI DC voltage used low-pass filters

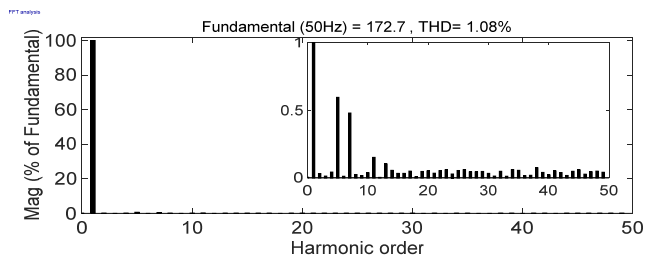


Fig.14. Frequency spectrum of source current for fixed band hysteresis and fuzzy DC voltage used low-pass filters

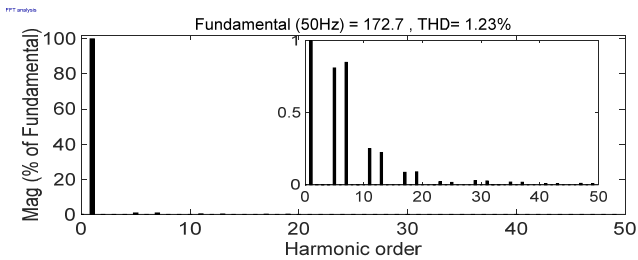


Fig. 15. Frequency spectrum of source current for fuzzy band hysteresis and PI DC voltage used low-pass filters

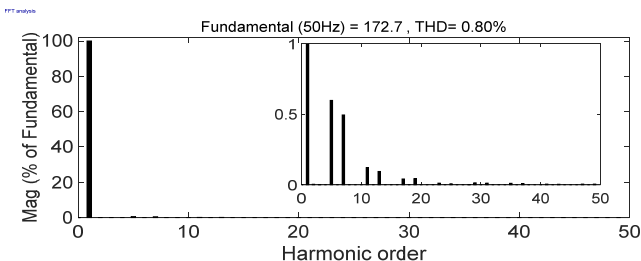


Fig. 16. Frequency spectrum of source current for fuzzy band hysteresis and fuzzy DC voltage used low-pass filters

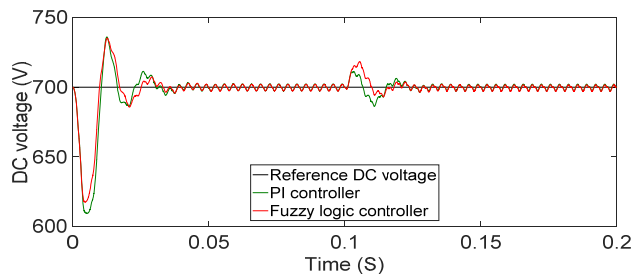


Fig. 17. DC bus voltage responses with a PI regulator and a fuzzy logic controller used low-pass filters

Figure 11 shows that the deformation of the line current has been corrected following the intervention of the SAPF. From the zoom performed on the spectral representations of the line current, the fixed band hysteresis current control technique generates additional harmonics of small amplitudes, unlike the fuzzy band hysteresis current control, which generates no additional harmonic.

The waveform of the current injected by the SAPF is illustrated in Fig. 12, where it is possible to observe the adaptation capacity of the SAPF during a disturbance in the load. The zooms performed on these figures show that the combination of fuzzy logic theory with the hysteresis current control strategy has eliminated the ripples of the line current. Effectively, the fuzzy band hysteresis improves the filtering performance of the SAPF by reducing the error between the reference current generated by the identification method and the current that the SAPF is injected on the grid.

Figures 13 and 15 shows that the application of the fuzzy band hysteresis current control technique has further improved the harmonic content of the line current by decreasing the THD from 1.34% to 1.23%

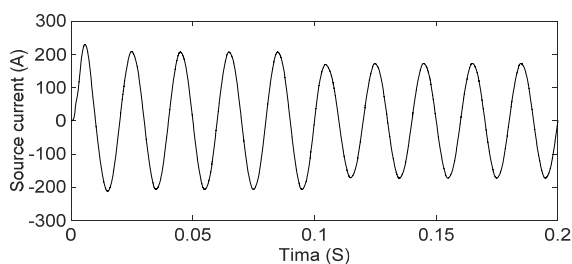


Fig. 18. Waveform of the source current used ADALINE filters and fuzzy band hysteresis

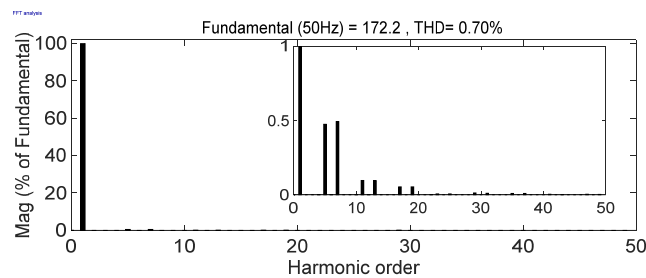


Fig. 19. Frequency spectrum of source current for fuzzy band hysteresis and fuzzy DC voltage used ADALINE filter

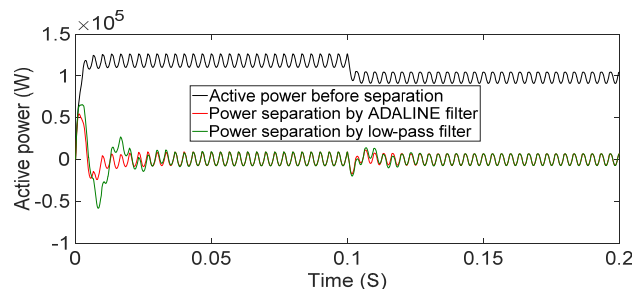


Fig. 20. Active power separation with ADALINE filters and low-pass filter

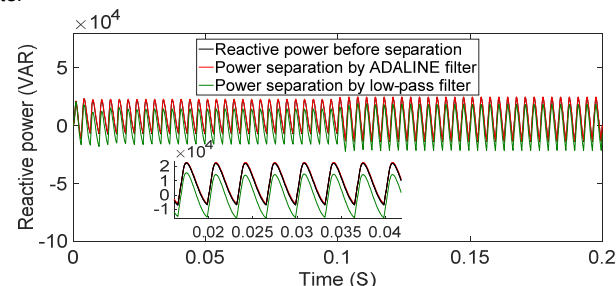


Fig. 21. Reactive power separation with ADALINE filters and low-pass filter.

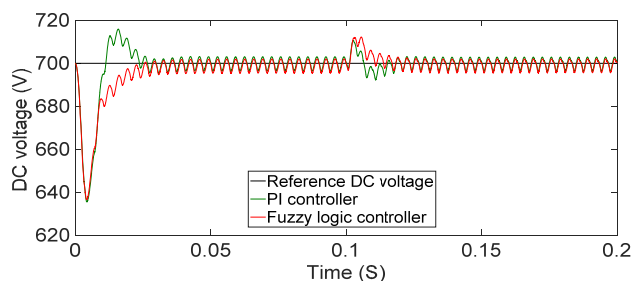


Fig. 22. DC bus voltage responses with a PI regulator and a fuzzy logic controller used ADALINE filters

The results obtained correspond to a control of the DC voltage by a PI regulator. The use of a fuzzy logic controller allowed, according to Figs. 14, 16 and 17, to reduce the THD of the line current from 1.08% to 0.80%. The efficiency of the fuzzy logic controller can be clearly seen in Fig. 17 where the response of the DC voltage controlled by a fuzzy regulator is better compared to that of a PI regulator in terms of stability and rapidity.

For Adaline Neural Network can be seen that with this method it is possible to estimate the harmonics individually and all harmonic currents considered in the inputs of the two ADALINE. The results obtained by the proposed ANN-RIIP extraction method have showed a great efficiency in harmonic identification. The waveforms show the measured load current before compensation, Fig. 10 with THD =12.64%. After the filtering used the ADALINE filter for harmonic extraction and the fuzzy hysteresis band technique for inverter modulation stability control and DC fuzzy controller to ensure DC voltage stability. We have given a very high

development term of THD =0.7 fig.19 with a very efficient compensation of the reactive energy.

It is simple to calculate and allows a good dynamic response time, particularly when implementing the Neural-RIIP theory, which uses two adaline filters in place of a low-pass filter. The THD decreased from 12.64% to 0.7% meaning that in the case used ADALINE filters in place of low pass filters the THD decreased from 0.8%, to 0.7% figs.16, 19. The weak points of RIIP theory classic are the delay created by the low pass filter and the fact that it is limited to provide good filtering performance in the case of a balanced sinusoidal voltage system.

The separation of the active and reactive power which is made by the ADALINE technique shows a very clear improvement between the low-pass filter and the other ADALINE filter used, in the active power separated by the ADALINE filter gives a fast response time and less amplitude disturbances on the other hand the low-pass filter shows a large amplitude disturbance and slow response time compared to the ADALINE filter fig.20. For the reactive power, the ADALINE filter used gives a better compensation than the low-pass filter fig.21

Fuzzy control of the DC voltage has resulted in good disturbance rejection compared to a PI controller (Fig.22), especially when using the ADALINE filter for harmonic extraction.

Table 4. THD values of the source current for the different techniques used

Without APF		
THD of source current Without load variation		THD of source current with load variation
9.02%		12.64%
With APF		
classical RIIP method	BandeFixe Vdc_PI	1.34%
	BandeFixe Vdc_fuzzy logic	1.08%
	Bande Floue/ Vdc_PI	1.23%
	BandeFloue Vdc_fuzzy logic	0.8%
neural-RIIP method	BandeFloue Vdc_fuzzy logic	0.7%

Conclusion

In this paper, several control techniques have been discussed. These are the identification of harmonics by the classical RIIP and neural-RIIP theory, the fixed band and fuzzy band hysteresis control technique for current control and the use of a fuzzy logic controller for DC voltage control. In order to show the effectiveness of the proposed strategies, simulation tests were carried out under the conditions of a non-linear load variation. The results obtained show an improvement in the performance of the shunt active power filter in terms of current control. The fixed-band hysteresis current control provides a fast response but generates excessive current ripple due to the variable modulation frequency. This problem was solved using a fuzzy hysteresis band current control technique, which allowed the system to achieve good active filtering and minimize ripple and harmonic distortion of the line current. Fuzzy control of the DC voltage has resulted in good disturbance rejection compared to a PI controller, especially when using the ADALINE filter for harmonic extraction, and a satisfactory improvement in harmonic distortion of the current. ADALINE networks are linear estimators capable of learning signals on-line as a function of time. The learning is fast and robust while being compatible with a real-time constraint; moreover, the simplicity of its architecture gives it additional advantages: the interpretation of its weights and

the lower harmonic reduction of 5% as required by the standards.

Acknowledgement

This project was financially supported by the Directorate General for Scientific Research and Technological Development - Algerian Ministry of Higher Education and Scientific Research of Algeria.

Authors: Khenfar noureddine, ICEPS Laboratory, phd student Sciences Faculty, Electrical Engineering Department, Djillali Liabes University of Sidi Bel Abbes 22000, Algeria..E-mail : khenfar.noureddine@gmail.com.

REFERENCES

- [1] A. CHAOUI, J.-P. GAUBERT, A. BOUAFIA, "Experimental validation of new direct power control switching table for shunt active power filter power", conference on Electronics and Applications (EPE), 2013
- [2] R. BELAÏDI, M. HATTI, A. HADDOUCHE, M. M. LARAFI, "Shunt active power filter connected to a photovoltaic array for compensating harmonics and reactive power simultaneously", 4th international conference on power engineering, energy and electrical drives, may 2013
- [3] B. SINGH, K. AL-HADDAD, A. CHANDRA, "A review of active filters for power quality improvement", IEEE transactions on industrial electronics, vol. 46, no. 5, October 1999
- [4] G. W. CHANG, C. M. YEH, "Optimisation-based strategy for shunt active power filter control under non-ideal supply voltages", IEEE proceedings - electric power applications, vol. 152, no. 2, pp. 182, 2005
- [5] H. AKAGI, E. HIROKAZU, WATANABE, M. AREDES, "Instantaneous power theory and application to power conditioning", USA: IEEE Press 200
- [6] N. MESBAHI, AOUARI, D. OULD ABDESLAM, T. DJAMAH, AOMEIRI, "Direct power control of shunt active filter using high selectivity filter (HSF) under distorted or unbalanced conditions", electric power systems research 108 (2014) 113-123
- [7] GHADBANE Ismail BENCHOUIA Mohamed Toufik BARKAT Said "Real time implementation of feedback linearization control based three phase shunt active power filter", European Journal of Electrical Engineering – n° 4/2018, 1-5
- [8] B. MAZARI, F. MEKRI, "Fuzzy hysteresis control and parameter optimization of a shunt active power filter", journal of information science and engineering 21, 1139-1156 (2005)
- [9] Larbi Hamiche¹, Salah Saad^{*1}, Leila Merabet¹ & Fares Zaamouche² "Adaline Neural Network and Real-Imaginary Instantaneous Powers Method for Harmonic Identification La méthode réseau de neurone Adaline et puissances instantanées réels imaginaires pour l'identification des harmoniques", Rev. Sci. Technol., Synthèse 36: 129-140 (2018)
- [10] Kadem, M., Semmah, A., Wira, P., & Slimane, A. (2020). Artificial Neural Network Active Power Filter with Immunity in Distributed Generation. Periodica Polytechnica Mechanical Engineering. doi:10.3311/ppme.12775
- [11] Abdeslam, D. O., Wira, P., Merckle, J., Flieller, D., & Chapuis, Y.-A. (2007). A Unified Artificial Neural Network Architecture for Active Power Filters. IEEE Transactions on Industrial Electronics, 54(1), 61–76. doi:10.1109/tie.2006.888758
- [12] F. Merki "Commande robuste des conditionneurs Actifs de puissances," thèse de doctorat, USTO, 2007
- [13] Loutfi, B. (2019). Comparative analysis hysteresis and fuzzy logic hysteresis controller of shunt active filter. Advances in Modelling and Analysis B, Vol. 62, No. 2-4, pp. 37-42. https://doi.org/10.18280/ama_b.622-401
- [14] Georgios A. Tsengenes and al. « Performance Evaluation of PI and Fuzzy Controlled Power Electronic Inverters for Power Quality Improvement ». Chapter from the book Fuzzy Controllers - Recent Advances in Theory and Applications
- [15] Rathika, P., Devaraj, D. (2010). Fuzzy logic based approach for adaptive hysteresis band and dc voltage control in shunt active filter. International Journal of Computer and Electrical Engineering, 2(3): 1793-8163